Supporting Information

Highly effective Ir-based catalysts for the benzoic acid hydrogenation: experiment and theory guided catalysts rational design

*Minghui Tang[+], Shanjun Mao[+], Xuefeng Li, Chunhong Chen, Mingming Li, and Yong Wang**

Advanced Materials and Catalysis Group, ZJU-NHU United R&D Center,

Department of Chemistry, Zhejiang University, Hangzhou 310028, P. R.China.

*Corresponding author

Fax: (+) 0571-8795-1895, E-mail: chemwy@zju.edu.cn

Contents

Experimental section

1. Hot filtration test

A hot filtration test was carried out by stopping a standard BA hydrogenation catalyzed by Ir/CN after 1 hour and passing the reaction mixture through a sintered discs filter. The reaction liquid was returned to the reaction vessel and continued to react. No further substrate conversion in the filtrate occurred after catalyst removal at the reaction temperature, indicating that the Ir is strongly bound to the support surface and no significant quantities of metal are lost to the reaction liquid during the process.

2. The reusability of the catalyst.

In a typical process, after a recycle, the catalyst was separated from the reaction mixture by centrifugation, thoroughly washed with ethanol, dried at 70 °C, and then reused as the catalyst in subsequent runs under identical reaction conditions.

3. The calculation formula of TOF in the hydrogenation reaction:

$$TOF_M = \frac{\text{the moles of BA conversion}}{\text{the moles of metal} \times \text{reaction time}}$$

M: metal

Table S1. Catalytic results of Pd/CN and other Pd catalysts form ref.9 [1] [a]

Entry	Catalyst	Yield (%)	TOF (h^{-1})
1	Pd/CN	100	0.883
2	Pd/TiO_2	10	0.088
3	Pd/CeO_2	13	0.115
4	Pd/MgO	0	-
5	$Pd/\gamma\text{-}Al_2O_3$	21	0.186
6	Pd/AC	11	0.097
7	$Pd/CN_{0.132}$	81	0.716
8	Pd/HC	14	0.124

[a] Reaction conditions: benzoic acid 61 mg (0.5 mmol), catalyst (5 wt.% Pd) 50 mg, solvent water 25 mL, 85 °C, H_2 1 bar, 24 h

Table S2. Catalytic results for different catalysts form ref.1 [2] [a]

Entry	Catalyst	Yield %
1	RuPd/CN	67
2	RuPd/HC	28
3	RuPd/AC	45
4	RuPd/CNT	39

[a] Reaction conditions: BA 0.5 mmol, catalyst 50 mg, solvent water 25 mL, 85 °C, 0.1MPa H_2, 6 hours.

Table S3. Comparison of the catalytic activities for the Ir-based catalysts system with the prior Pt-group catalysts system under mild reaction conditions.

Entry	Precatalyst	Conditions	TOF(h^{-1})
		T(°C)/P_{H2}(MPa)/Solvent	
1	Rh/C	60°C/0.1 MPa/iPrOH	0.38 [3]
2	Pt+$AlCl_3$	60°C/0.1 MPa/H_2O	2.03 [4]
3	Pd@CN	85°C/0.1 MPa/H_2O	0.883 [5]
4	Pd@γ-Al_2O_3	85°C/0.1 MPa/H_2O	0.186 [5]
5	Ru/CN	85°C/0.1 MPa/H_2O	0.31 [2]
6	Pd/AC	85°C/0.1 MPa/H_2O	2.1 [6]
7	Ir/AC	85°C/0.1 MPa/H_2O	19 (this work)
8	Ir/CN	85°C/0.1 MPa/H_2O	34 (this work)
9	Ir/γ-Al_2O_3	85°C/0.1 MPa/H_2O	40 (this work)
10	Ir/CN	55°C/1.0 MPa/H_2O	57 (this work)
11	Ru/C	60°C/0.5 MPa/iPrOH	0.36 [3]
12	Pt nanowires	70°C/1.0 MPa/Acetic acid	5.3 [7]
13	Pd/AC	85°C/1.5 MPa/H_2O	5.7 [6]
14	Pd/CNF	85°C/1.5 MPa/H_2O	2.83 [6]
15	Pd/CNF	85°C/1.5 MPa/H_2O	0.35 [8]
16	Pd/AC	85°C/2.5 MPa/H_2O	3.9 [9]
17	Pd/NAC	85°C/2.5 MPa/H_2O	26 [9]
18	Pd/MCN	85°C/2.5 MPa/H_2O	55 [9]

Table S4. Specifications of different supports.

Material	S_{BET} (m^2g^{-1})	Pore volume (cm^3g^{-1})	Pore size (nm)
γ-Al_2O_3	120	0.77	204
TiO_2	7.3	0.03	214
CeO_2	6.0	0.04	157
ZrO_2	59	0.06	2.8
SBA-15	557	1.02	7.8
CN	211	0.67	10.7
AC	948	0.79	4.7

Table S5. The salient statistics of various Pt group metals for United States in 2015.[a]

Metal	Price /dollars per troy ounce
Pt	1080.00
Pd	690.00
Rh	970.00
Ir	530.00
Ru	48.00

[a] Information Source: USGS (United States Geological Survey). Minerals Information[EB/OL]. [2015-01-22]. http://minerals.usgs.gov/minerals/pubs/commodity/.

Table S6. Catalytic results for different catalysts [a]

Catalyst	Conv. (%)	Sel. (%)	TOF (h-1)
Rh/CN	33	100	86
Ir/CN	27	100	69
Pt/CN	30	100	47
Pd/CN	6	100	4
Ru/CN	25	100	20

[a] Reaction conditions: benzoic acid 1 mmol, catalyst (5 wt.% Ir) 25 mg, solvent water 25 mL, 55 ^{o}C, 0.4MPa H_2.

Table S7. Hydrogenation of BA over various Ir-based catalysts in different Solvents [a]

Entry	Catalyst	Solvent	Conv. (%)
1	Ir/γ-Al_2O_3	hexane	9
2	Ir/AC	hexane	7
3	Ir/CN	hexane	3
4	Ir/CN	water	33

[a] Reaction conditions: benzoic acid 0.5 mmol, catalyst (5 wt.% Ir) 50 mg, solvent 25 mL, 65 ^{o}C, H_2 1 bar, 1 h.

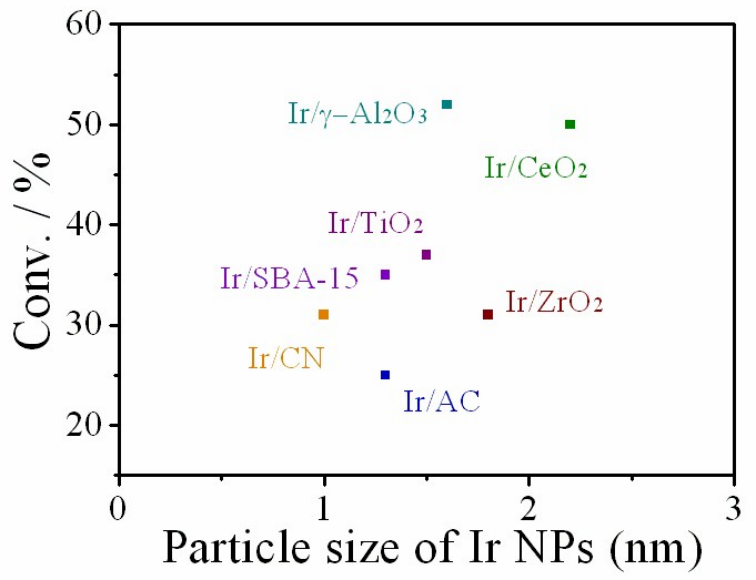

Figure S1. Relationship between BA conversion (the data were taken from Table 1) and particle size of Ir NPs of various catalysts.

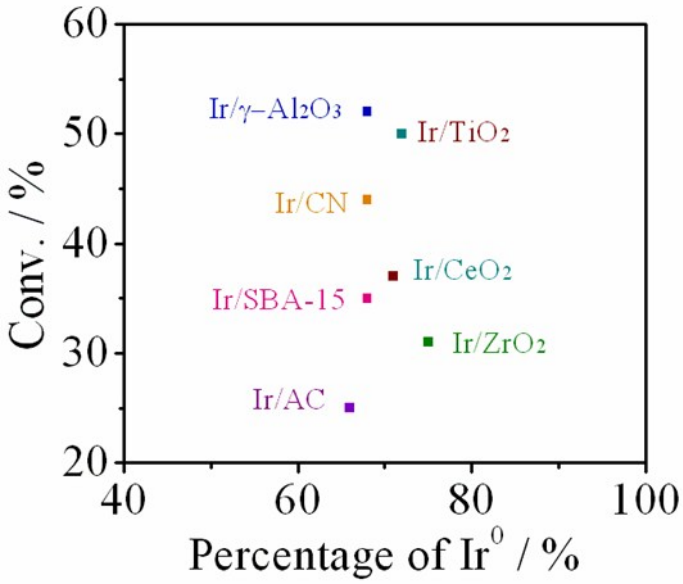

Figure S2. Relationship between BA conversion (the data were taken from Table 1) and percentage of Ir^0 in the Ir-based catalysts.

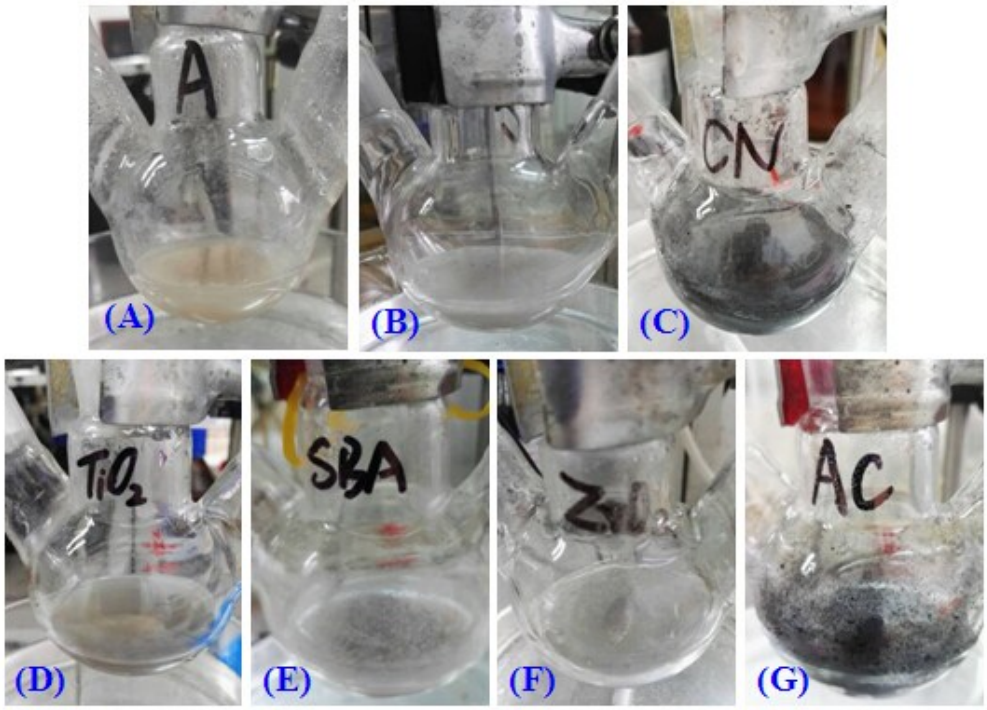

Figure S3. The reaction solutions with different catalysts (A) Ir/γ-Al_2O_3, (B) Ir/CeO_2, (C) Ir/CN, (D) Ir/TiO_2, (E) Ir/SBA-15, (F) Ir/ZrO_2, (G) Ir/AC after reaction for 0.5 h

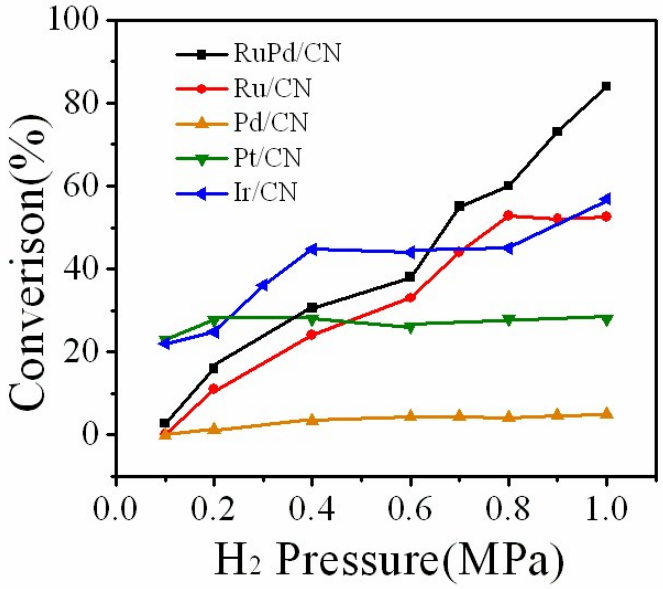

Figure S4. Influence of hydrogen pressure on BA conversion with different catalysts. Reaction conditions: BA 1 mmol, catalyst 25 mg, water 25 mL, 55 °C, 1 h.

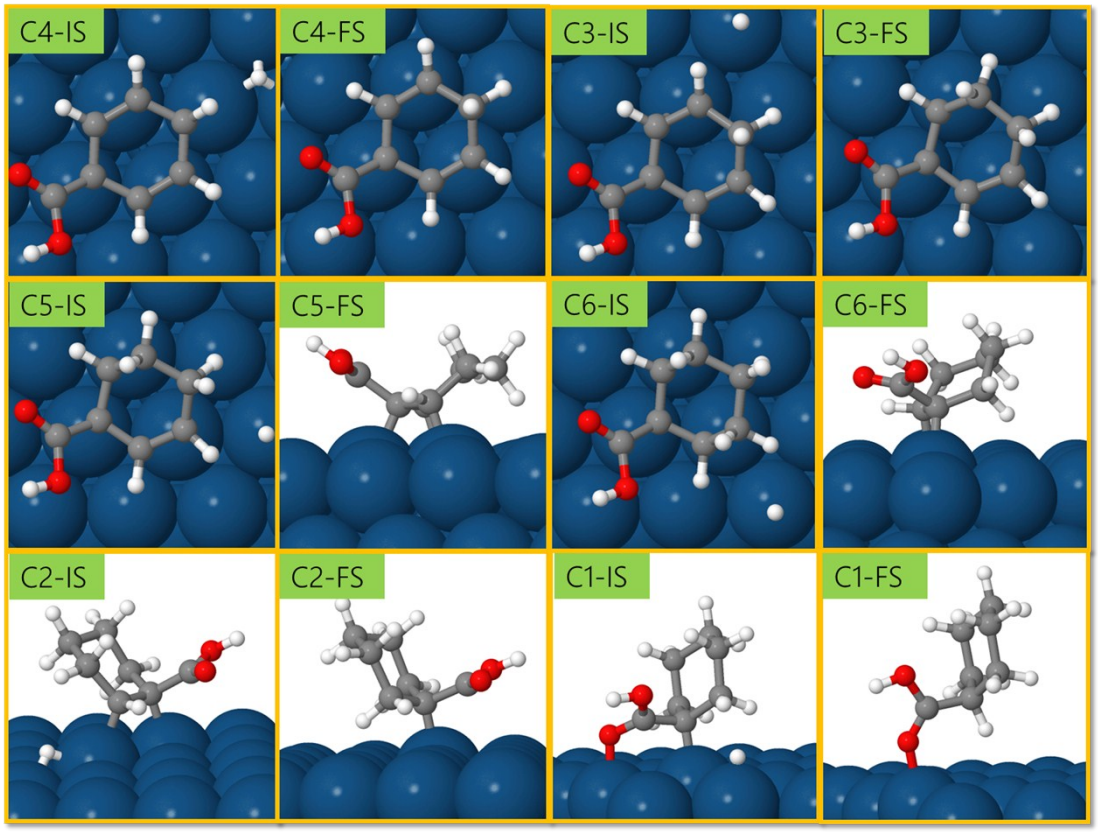

Figure S5. The initial and final structure for each hydrogenation step along the hydrogenation pathway beginning with C4 site

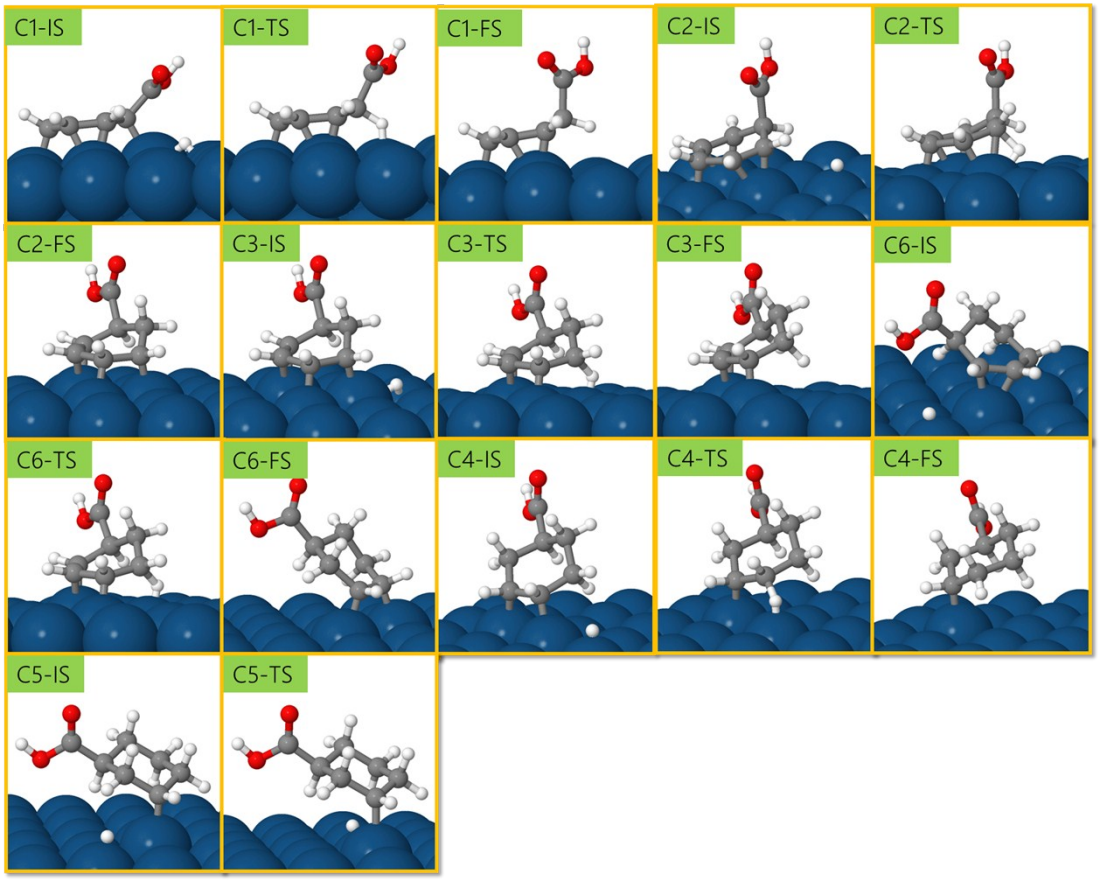

Figure S6. The related structures beginning with C1 site. IS: initial state; TS: transition state; FS: final state.

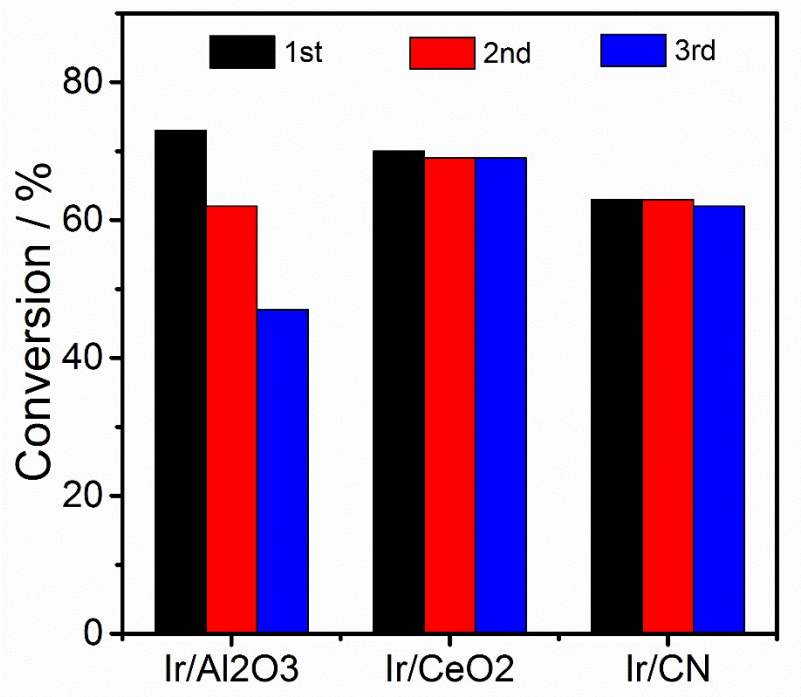

Figure S7. Comparison of the reusability of the Ir/Al_2O_3, Ir/CeO_2 and Ir/CN in the BA hydrogenation under the same reaction conditions. Reaction conditions: BA 200 mg, cat 100 mg, solvent water 25 mL, 55°C, 0.5 MPa H_2, 1h.

We investigated the reusability of the Ir/Al_2O_3, Ir/CeO_2, and Ir/CN, respectively. After easy separation and pretreated, Ir/CeO_2 and Ir/CN still could keep high performance for three cycles. However, for Ir/Al_2O_3, there was a considerable decrease in catalytic activity during three recycling tests.

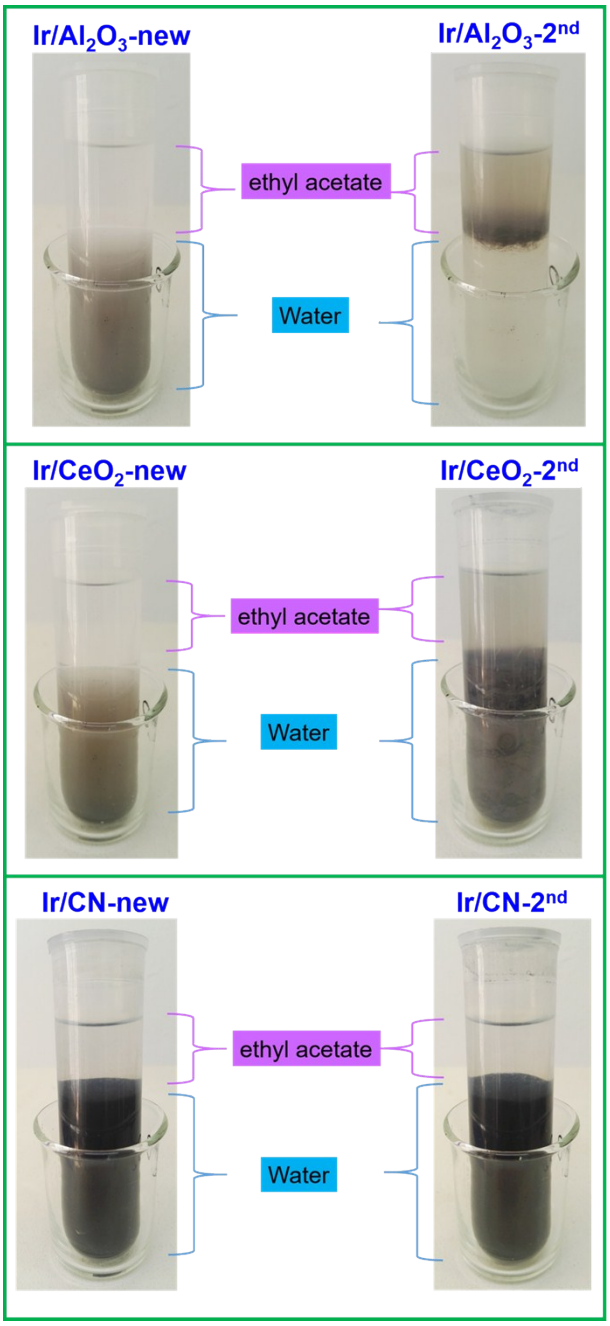

Figure S8. The catalysts dispersion in two-phase solvent system, the upper was ethyl acetate, the bottom was water.

We have noticed an interesting phenomenon during the recycling experiments. Specifically, all catalysts can disperse well in water at the first reaction. It was found that after two recycle reactions, the reused Ir/Al_2O_3 was more inclined to disperse in ethyl acetate, but the reused Ir/CeO_2 and Ir/CN were dispersed well in water.

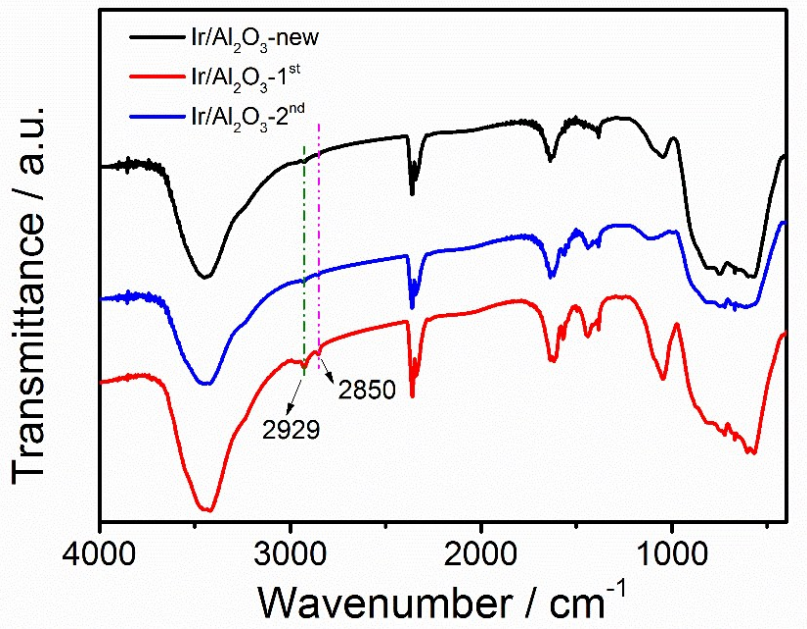

Figure S9. FTIR spectra of the Ir/Al_2O_3 before and after reaction.

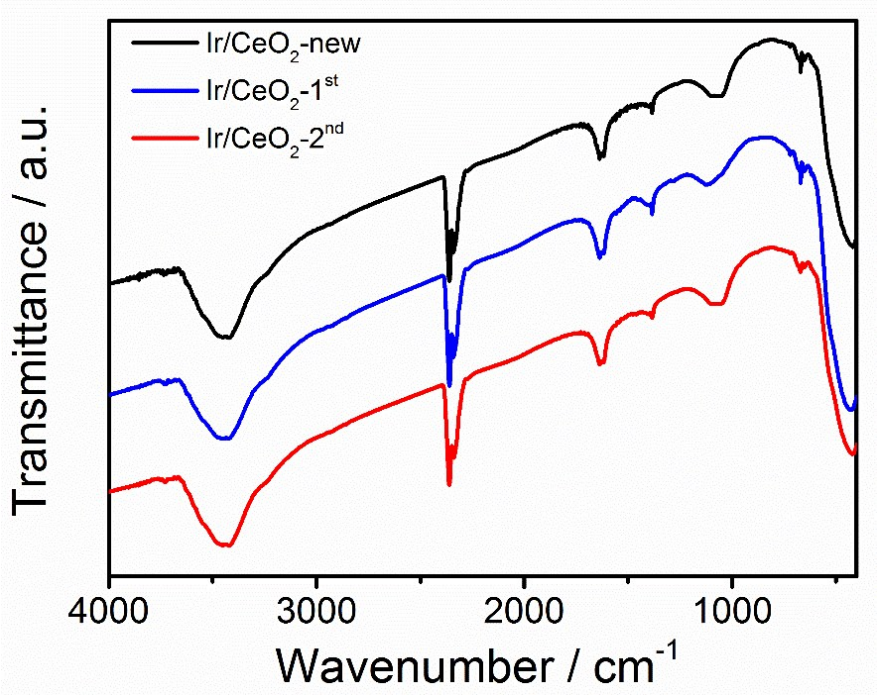

Figure S10. FTIR spectra of the Ir/CeO_2 before and after reaction.

The FTIR experiments have been performed. According to FTIR spectra of fresh and recoverd Ir/Al_2O_3 (Figure S9), it can be seen that after first reaction, two peaks at 2929 and 2850 cm^{-1} were appeared on recovered Ir/Al_2O_3 (Ir/Al_2O_3-2^{nd}), and the peak intensity was also strengthened after second reaction (Ir/Al_2O_3-3^{rd}). The peaks at 2929

and 2850 cm^{-1} could be assigned to C-H stretching vibrations of the cyclohexanecarboxylic acid adsorbed on the catalyst surface.[10] As a result, some of the benzoic acid hydrogenation product cyclohexanecarboxylic acid was adsorbed on the surface of recovered Ir/Al_2O_3, which might hinder the catalyst dispersion in water and occupy the active sites , thereby decreasing the catalytic performance significantly.

As a comparison, the FTIR spectra of the fresh and recoverd Ir/CeO_2 showed no obvious difference (Figure S10). Therefore, the Ir/CeO_2 can resist the poison of cyclohexanecarboxylic acid and maintain high performance.

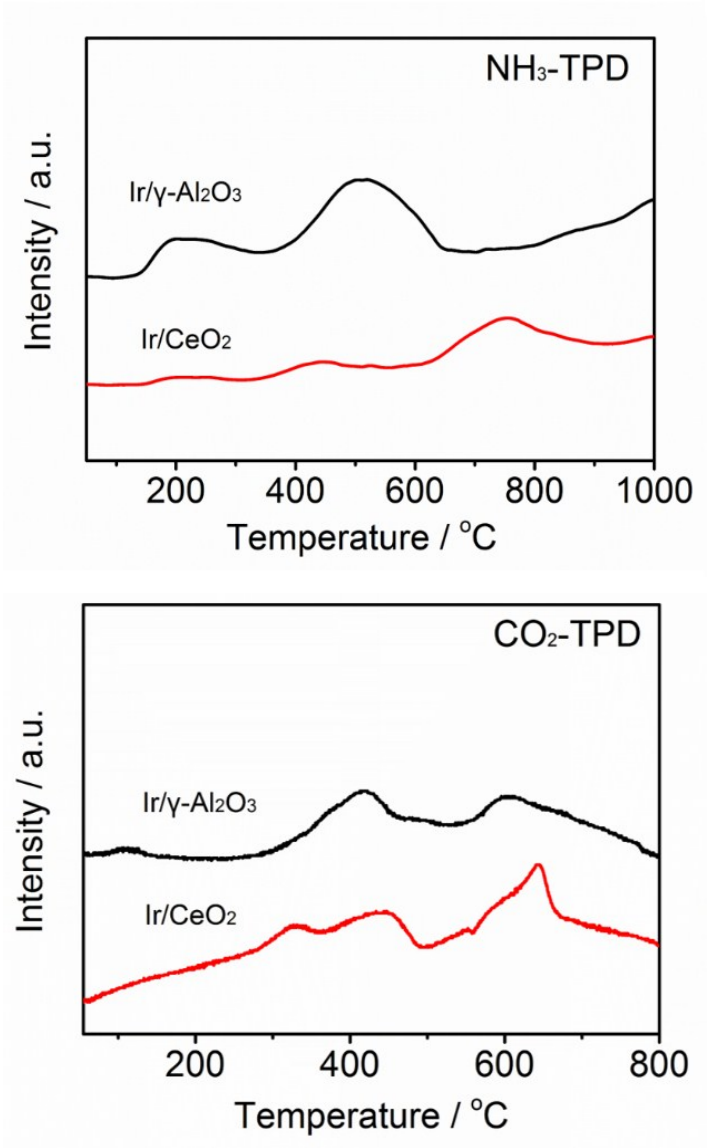

Figure S11. NH_3-TPD and CO_2-TPD patterns of Ir/γ-Al_2O_3 and Ir/CeO_2.

From the results of Table 1 in the manuscript, the catalytic performance of Ir/γ-Al_2O_3 and Ir/CeO_2 was almost the same, 52% BA conversion for Ir/γ-Al_2O_3, and 50% BA conversion for Ir/CeO_2. NH_3-TPD and CO_2-TPD experiments were performed to study the surface acidity and basicity of these two catalysts, respectively. The results were shown as Figure S11.

In the NH_3-TPD patterns, the Ir/γ-Al_2O_3 presents two desorption peak of NH_3 with maxima at about 208 and 517 °C, demonstrating that two types of acid site distributed on the surface of Ir/γ-Al_2O_3. For the Ir/CeO_2, only a desorption peak of NH_3 with maxima at about 756 °C was obvious observed. In addition, the adsorption

of NH_3 on Ir/CeO_2 was lower than that of $Ir/\gamma\text{-}Al_2O_3$, thus demonstrating that the amount of acid site on Ir/CeO_2 were lower than that of $Ir/\gamma\text{-}Al_2O_3$.

In the CO_2-TPD patterns, the $Ir/\gamma\text{-}Al_2O_3$ presents two desorption peak of CO_2 with maxima at about 418 and 607 ^oC. Whereas, the Ir/CeO_2 presents three desorption peak of CO_2 with maxima at about 323, 447 and 644 ^oC. These results demonstrated that the strength and amount of surface basic site for $Ir/\gamma\text{-}Al_2O_3$ and Ir/CeO_2 were also different.

Therefore, although the acid and basic sites were different for Ir/CeO_2 and $Ir/\gamma\text{-}Al_2O_3$, their catalytic performance were almost the same. So the distribution of acid and basic sites on $\gamma\text{-}Al_2O_3$ was not responsible for the highest activity shown by the $Ir/\gamma\text{-}Al_2O_3$ catalysts.

References

[1] X. Xu, Y. Li, Y. Gong, P. Zhang, H. Li, Y. Wang, Synthesis of Palladium Nanoparticles Supported on Mesoporous N-Doped Carbon and Their Catalytic Ability for Biofuel Upgrade, J. Am. Chem. Soc., 134 (2012) 16987-16990.
[2] M. Tang, S. Mao, M. Li, Z. Wei, F. Xu, H. Li, Y. Wang, RuPd Alloy Nanoparticles Supported on N-Doped Carbon as an Efficient and Stable Catalyst for Benzoic Acid Hydrogenation, ACS Catalysis, 5 (2015) 3100-3107.
[3] T. Maegawa, A. Akashi, K. Yaguchi, Y. Iwasaki, M. Shigetsura, Y. Monguchi, H. Sajiki, Efficient and Practical Arene Hydrogenation by Heterogeneous Catalysts under Mild Conditions, Chemistry – A European Journal, 15 (2009) 6953-6963.
[4] T. Yu, J. Wang, X. Li, X. Cao, H. Gu, An Improved Method for the Complete Hydrogenation of Aromatic Compounds under 1 Bar H2 with Platinum Nanowires, ChemCatChem, 5 (2013) 2852-2855.
[5] X. Xu, M. Tang, M. Li, H. Li, Y. Wang, Hydrogenation of Benzoic Acid and Derivatives over Pd Nanoparticles Supported on N-Doped Carbon Derived from Glucosamine Hydrochloride, ACS Catalysis, 4 (2014) 3132-3135.
[6] J.A. Anderson, A. Athawale, F.E. Imrie, F.M. Mkenna, A. Mcue, D. Molyneux, K. Power, M. Shand, R.P.K. Wells, Aqueous phase hydrogenation of substituted phenyls over carbon nanofibre and activated carbon supported Pd, Journal of Catalysis, 270 (2010) 9-15.
[7] Z. Guo, L. Hu, H.-h. Yu, X. Cao, H. Gu, Controlled hydrogenation of aromatic compounds by platinum nanowire catalysts, RSC Advances, 2 (2012) 3477-3480.
[8] J. Anderson, F.-M. McKenna, A. Linares-Solano, R.K. Wells, Use of Water as a Solvent in Directing Hydrogenation Reactions of Aromatic Acids over Pd/carbon Nanofibre Catalysts, Catal. Lett., 119 (2007) 16-20.
[9] H. Jiang, X. Yu, R. Nie, X. Lu, D. Zhou, Q. Xia, Selective hydrogenation of aromatic carboxylic acids over basic N-doped mesoporous carbon supported palladium catalysts, Applied Catalysis A: General, 520 (2016) 73-81.
[10] J.-l. Yan, G.-j. Chen, J. Cao, W. Yang, B.-h. Xie, M.-b. Yang, Functionalized graphene oxide with ethylenediamine and 1,6-hexanediamine, New Carbon Materials, 27 (2012) 370-376.